EXPERIMENTS WITH HIGHLY CHARGED IONS AT THE PARIS ECR ION SOURCE, SIMPA*

C. I. Szabo, D. Attia, A. Gumberidze, P. Indelicato, E.-O. Le Bigot, S. Schlesser (LKB, Paris, France),
E. Lamour, J. Merot, C. Prignet, J.-P. Rozet, M. Trassinelli, D. Vernhet (INSP, Paris, France),
S. J. Coelho do Carmo (Coimbra University, Coimbra, Portugal)

Abstract

In this paper recent achievements will be reported at the SIMPA ion source in Paris that include the first use of an electrostatic ion trap for trapping highly charged ions on the beam line of an ECR ion source and electron temperature and density measurements with the help of the observation of the bremsstrahlung spectrum of the electrons in the ECR plasma of the source. Also a new vacuum double crystal spectrometer is under construction in our lab that will allow us to measure the very narrow inner shell transitions of highly charged ions produced in the ECR plasma and provide new x-ray standards with this method for the atomic physics community.

THE SIMPA ION SOURCE

The full permanent magnet "supernanogan" type Electron Cyclotron Resonance (ECR) ion source, SIMPA (Source d'Ions Multichargés de Paris = Paris highly charged ion sourcs) has been jointly operated by LKB (Laboratoire Kastler Brossel) and INSP (Institut des NanoSciences de Paris) since 2004. Since this time numerous projects have been started to use the extracted beam in atomic physics and surface physics experiments and the x-ray radiation of the ECR plasma for plasma and atomic physics investigations. The ion source has a fully permanent magnet setup with a microwave line of 14.5 GHz attached into the plasma chamber. The extraction is made possible by raising the whole ion source to a high voltage platform between 0 kV to 35 kV potential, leaving the beam line at ground potential. The beam line has a solenoid magnet for beam focusing. Charge state selection and scan is possible with a dipole magnet. Figure 1 shows a general setup of the SIMPA ECR ion source laboratory in Paris.

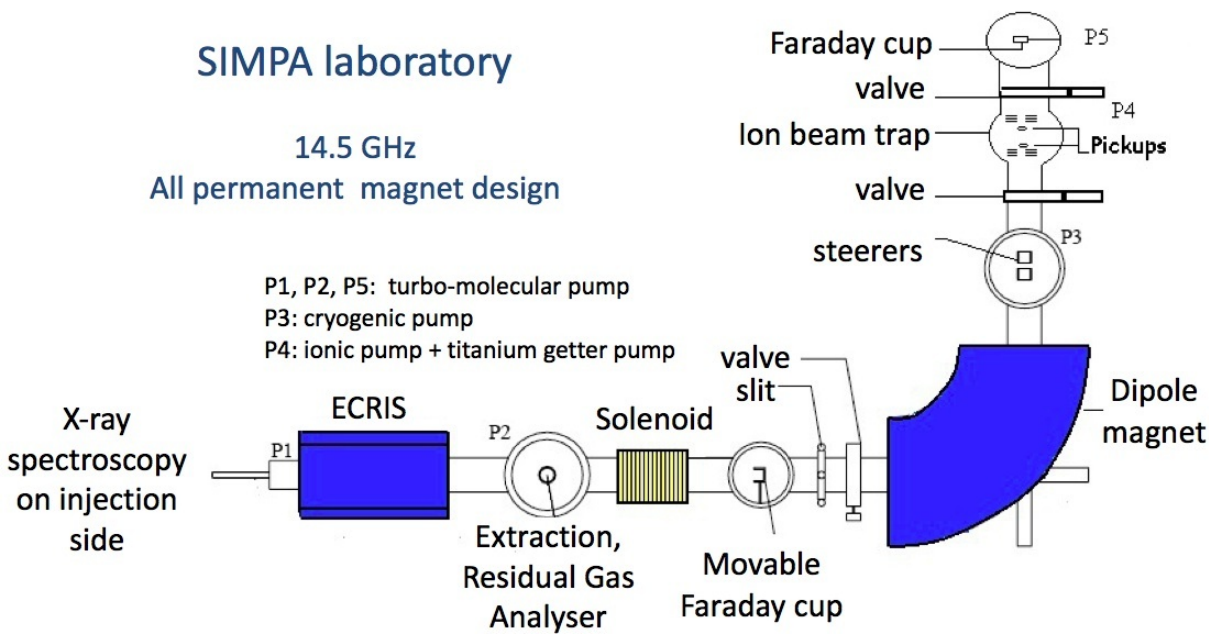

Figure 1: The SIMPA ECR Ion Source laboratory in Paris. The 14.5 GHZ all permanent magnet SUPERNANOGAN type ECR ion source is connected to a beam line with a solenoid and dipole magnet feeding the ion beam trap. A Be window on the injection side allows x-ray spectroscopy

THE ELECTROSTATIC ION BEAM TRAP

The development and applications of ion traps and heavy-ion storage rings have a significant impact on many branches of physics. These devices enable the storage of ions for a relatively long time, with meV to eV kinetic energies, in ion traps and to GeV kinetic energies, in heavy-ion storage rings. Ion traps are able to trap charged particles for a long time, and they have been successfully applied in several areas of physics. Recently,

a novel type of ion traps has been developed [1, 2], in which ions oscillate between a pair of electrostatic mirrors, much like photons in an optical resonator. The trapped ions have kinetic energies of a few keV per charge in the central part of the trap while inside the mirrors they have only a few meV near their turning points, where they are also subject to radial focusing forces. This means that this ion trap uses only electrostatic fields to trap a beam of ions, hence the name: electrostatic ion beam trap (EIBT). Several experiments have already been performed with these devices; such as lifetime measurements of singly charged ions [3, 4] and charge transfer dissociation of molecules [5]. Following a design from the Weizmann Institute [1], we have constructed an electrostatic ion beam trap and attached it to the beam line of SIMPA. Fig. 1 shows the ion trap on the beam line of the ion source. A schematic drawing of the trap together with a photo of the trap electrodes is displayed in Fig. 2.

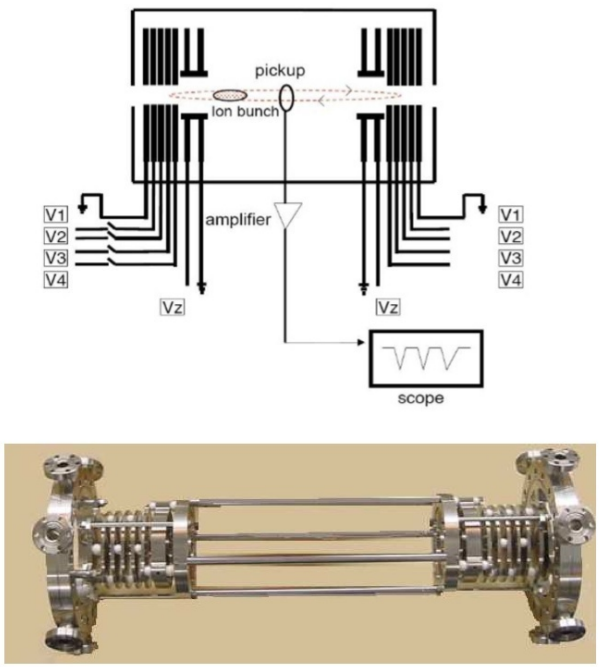

Figure 2: schematic view and a photo of the electrostatic ion trap on the beamline of SIMPA

The ion trap consists of two coaxial electrostatic mirrors, each composed of a stack of eight cylindrical electrodes. The configuration of the trap is characterized by the potentials on five of these electrodes, V1, V2, V3, V4, Vz (see Fig. 2), the other three electrodes are grounded. Provided that the field generated by these potentials fulfils certain criteria, ions can be trapped oscillating between the two mirrors [1]. A cryopump and an ion pump is pumping the trap to a pressure of about $5 \cdot 10^{-10}$ mbar. Injection of an ion bunch into the trap is performed by grounding all the entrance electrodes. The electrodes on the other side are kept at high potential so that the bunch is reflected toward the entrance. Before the ion bunch returns to the entrance mirror, the potentials of its electrodes are rapidly (<100 ns to 200 ns) raised and the ion bunch is thus confined between the mirrors. The highly charged ions are produced in the SIMPA ECR ion source and are extracted and accelerated by the extraction voltage of 4.2 kV. After extraction the ions are focused and analyzed by the solenoid and the dipole magnets and run into the electrostatic steerer where an electrostatic chopper creates bunches of ions with a temporal extension of 80 ns to 500 ns. (see fig. 1). The closure of the entrance of the trap is synchronized with this electrostatic chopper providing an adjustable delay making optimization possible. Also steering of the ions is possible with the other two electrostatic deflectors in the steerer region. The evolution of ion bunches during storage was monitored with a cylindrical pickup electrode with a length of 7 mm and an inner diameter of 18 mm located at the center of the trap (see fig. 2). The amplified pickup signal was recorded on a digital oscilloscope and a spectrum analyzer.

Experimental data and simulations for the electrostatic ion beam trap

With the help of the pick up electrode in the linear center of the trap we have proved trapping for tens of milliseconds in the case of a variety of high charge states of O, Ar, Kr and Xe ions (up to O^{5+}, Ar^{13+}, Kr^{21+} and Xe^{20+}). Using a low (< 20 V) radio frequency voltage with frequencies close to the oscillation frequency of the ions in the trap we were able to observe trapping times up to 50 ms. Running the ion trap in the so called ”bunching” or synchronization mode [2] in the time domain of the pickup signal we observed a strange oscillation on the millisecond scale superposing the ion oscillation in the trap on the microsecond scale. This is shown in Figure 3 for the case of Ar^{8+}.

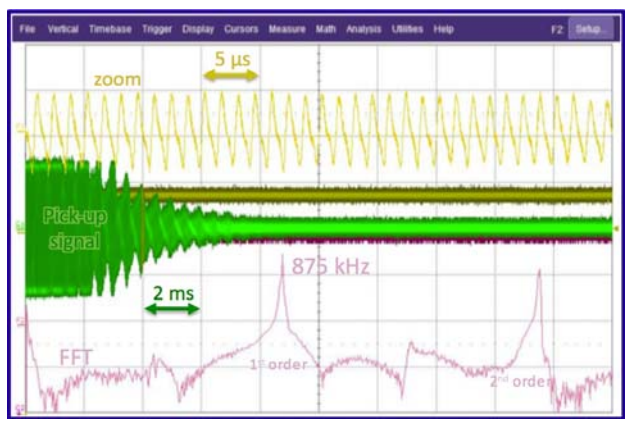

Figure 3: The screen of a digital oscilloscope showing trapping of Ar^{8+} ions. A zoom of a 20 µs region in time is shown on the top of the screen at 4 ms of trapping. The FFT of the oscillation (shown on the bottom) provides the trapping frequency: 875 kHz for Ar^{8+} at 4.2 keV kinetic energy per charge.

Our goal is to explain the observed oscillations with computer simulations. We mainly use two types of simulations for this purpose. The first method is based on

a 1D model described by Pedersen et al [6], where the behavior of a test ion close to a bunch of ions in the trap is investigated. The estimate for the bunch size dynamics can be obtained from observing variation of the distance between the test ion and the ion cloud as a function of time. This is shown in figure 4a, where millisecond scale oscillations of the bunch size is clearly visible. This could in principle, be considered as a possible reason for the observed oscillations in the experiment because the change in the bunch size could affect the pickup signal.

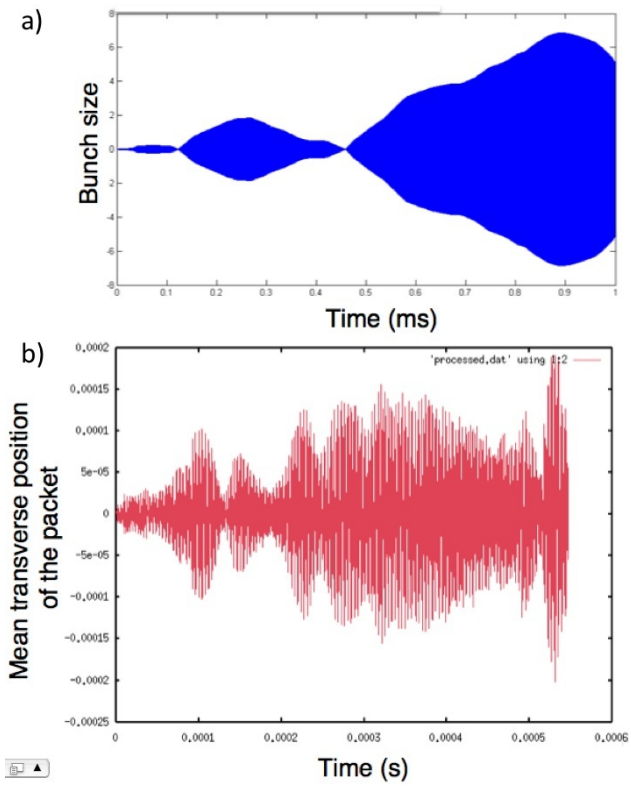

Figure 4: a) 1D simulation showing variation of the distance between the test ion and the ion cloud as function of time (bunch-size dynamics); b) N-particle 3D simulation of the bunch radial position as function of time.

In addition to the 1D model, we are developing an N-particle 3D simulation where we include the interaction between the ions fully and observe dynamics of all the particles in the potential of the trap. First results of this simulation are shown in fig 4b. Here, we show that if there is a slight misalignment during the injection of the ion beam in the trap, the radial velocity given to the bunch leads to radial oscillations of the packet. These radial oscillations could perturb the signal of the pickup as well because it depends on the distance from the charge. Further checks for various effects and consistency are underway. Now that we have proven trapping of highly-charged ions, we plan, as a next step, to utilize the ion trap for measurement of the life times of metastable states in highly charged ions.

ELECTRON TEMPERATURE MEASUREMENTS

We have used a silicon x-ray detector to observe bremsstrahlung radiation from the ECR ion source. The plasma was observed through the hollow polarization electrode on the injection side of the source, at a typical distance of 1 m. A 1 cm thick Pb collimator was used right in front of the detector with a 1 mm hole on it allowing x rays from the ion source to the detector. Pure aluminum filters were set in order to keep the rate on the Si(Li) detector on a reasonable level to avoid pile-up and high dead times. Different gases were injected into the ion source: argon, krypton and xenon, as well as oxygen rare-gas mixture. Other components typically present in the source were nitrogen and water. The x rays emitted by the source had to traverse a 250 µm thick Be window and 29 cm of air and when necessary a variable thickness (2 mm to 20 mm) Al filter. The absolute efficiency of the detector as a function of energy has been carefully measured previously. The measurement has been extended to higher energies with the help of an ^{241}Am radioactive source using known line intensity ratios up to 60 keV [9]. The detector efficiency corresponds very closely to that of a 5.755± 0.350 mm thick crystal, with no dead zone and a 26.5± 0.5 µm thick Be window, which is close to the manufacturers' specification. Efficiency and absorption through filters and windows are corrected for, using a Mathematica code interpolating data from the NIST x-ray mass absorption coefficients [10]. The energy scale was calibrated using the same ^{241}Am radioactive source. On Figure 5 we present typical spectra obtained for Xe plasmas at different injected microwave powers, after correction for detector efficiency and filter absorption.

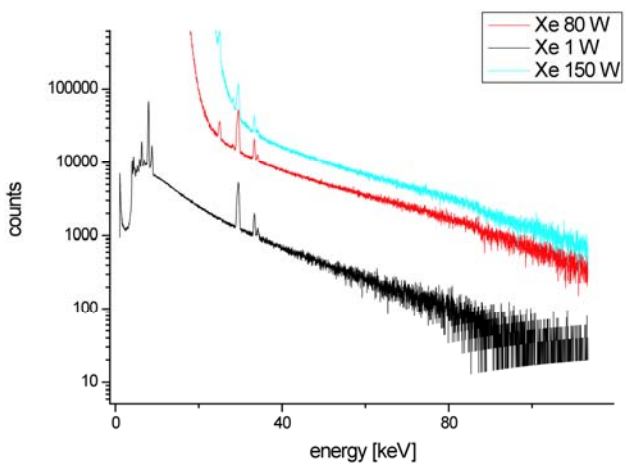

Figure 5: Examples of Xe x-ray spectra obtained with different microwave powers applied to the source. Each spectrum is corrected for detector efficiency, air, filter and window absorption. All spectra have been normalized by the acquisition time. Energy scale was obtained using an ^{241}Am source.

The bremsstrahlung tail clearly appears up to energies of 110 keV. To obtain the average electron temperature, we do a weighted fit of an exponential *AExp(-e/T)* to the spectra, for a range of energy between 40 keV and 110 keV.

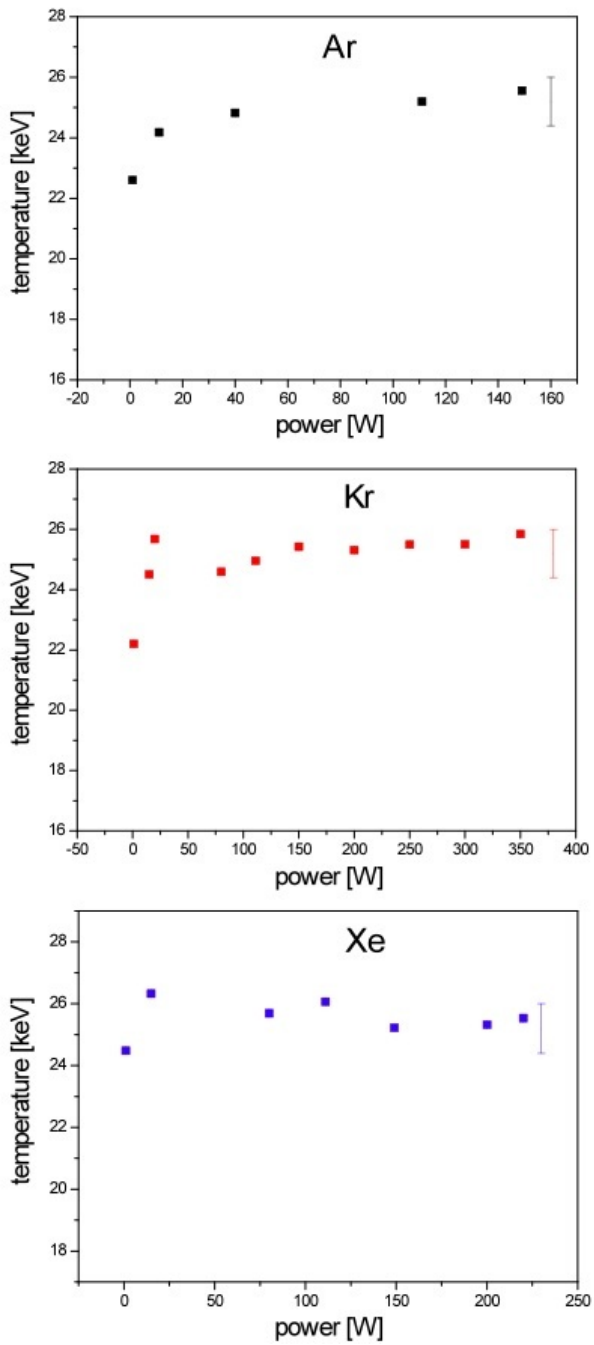

Figure 6: Maxwellian temperatures kT_{Mw} in keV, as a function of the microwave power in SIMPA in the case of different gases injected in the source.

The weighted fit is using the square root of the measured intensities in each point. A lower end for the fit was determined because the low energy part of the spectra after efficiency and absorption corrections is very intense. Even with filters that should cut the low energy part of the spectrum, one can observe an increase of the intensities after corrections. This increase is due to Compton scattering following escape of high-energy photons from the crystal, which leads to only a partial deposition of the original photon energy in the detector. These events produce high count-rates in the low energy part of the spectra that would modify the exponential fit if included. The upper limit of the fit corresponds to the place where the detector efficiency becomes too small and statistical uncertainty becomes too large. We have noticed that the correction for absorbers based on [10] did not completely consistently compensate for the absorber effect for different thicknesses and the calculated electron temperature values deviated from each other by up to 10%. A corresponding correction was applied based on the comparison of measurements for different Al absorber thicknesses with the one without an absorber, all of them carried out at 1 W (because for higher powers the photon rate was too high without absorbers). It was found that the effect increases with increasing absorber thickness. We attribute this effect to the fact that we do not have a "narrow" photon beam (=collimation is not ideal). This allows photons to get scattered in the absorber and the scattered photons hit the detector producing counts that are not taken into account when applying the corresponding absorber correction. A Monte Carlo simulation based on our experimental geometry has confirmed that this effect can for thick absorbers lead to the observed deviation of the resulting temperature. This deviation is included in the experimental error. On figure 6 we present the extracted spectral temperature as a function of microwave power for different gases (Argon, Krypton, Xenon). The error bars indicate systematic uncertainty due to the detector efficiency and the absorber corrections. The temperature changes initially at very low power and then practically saturates at about 25±1 keV average Maxwellian electron temperature. The starting temperature for Ar and Kr is around 22 keV and the saturation temperature of 25 keV is reached at powers around 100 W. For Xe however, the temperature is more or less constant. The saturation happens at lower power for lower-Z elements.

DOUBLE CRYSTAL X-RAY SPECTROMETER FOR X-RAY STANDARDS

A good way to understand the specific mechanisms that lead to the different charge state production and level populations in different ions is by the observation of the x-ray lines emitted by the ECR plasma, under different conditions, with a very high resolution. The K (2p → 1s) x-ray spectra of highly charged ions, emitted by an ECRIS, have been studied in a limited number of cases, on S, Cl, Ar, Co and Kr. [11]

Observation of x rays from 1+ to helium-like ions in S, Cl and Ar where performed with a spherically-bent, high-efficiency, Johann-type x-ray spectrometer, on the PSI

ECRIT [12] with a resolution ranging from 0.3 eV to 0.45 eV [13-17]. This increase in resolution, efficiency, and improvement in the background have lead to both high-accuracy x-ray measurements of few-electron highly-charged ions and to the observation of many unidentified lines, that should shed more light on the excited level population mechanisms, once the necessary analysis has been performed. Kα x rays from elements like argon are good probe of their ionization level in a plasma, because the electron undergoing the transition to the K shell for q>8 is in the same shell as the electron removed by the ionization process. Thus the shift in energy is large between charge states. The typical good resolution spectra from an Ar plasma contains an unresolved group of lines containing Kα lines from Ar^{+} to Ar^{9+} (i.e., ions with one K hole and 0 to 8 M holes), and then well resolved features from Ar^{10+} to Ar^{17+}, depending on the conditions of the plasma. Figure 7 shows good resolution (~3 eV) spectra of argon-oxygen mixture plasma, observed with a mosaic-graphite crystal spectrometer at the SIMPA source.

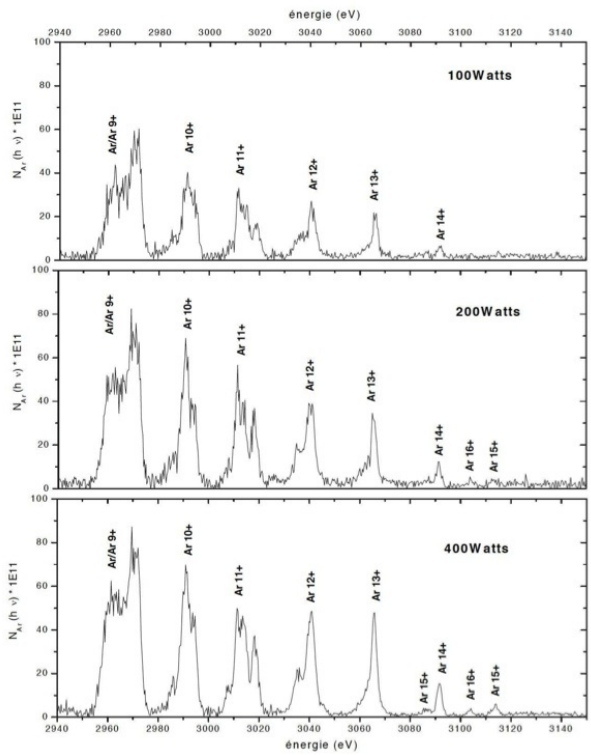

Figure 7: Normalized X-ray spectra of Ar ions in the plasma, as a function of microwave power, measured with a mosaic-crystal X-ray spectrometer.

These sample spectra are normalized and show clear change of the charge state distribution of the plasma with changing microwave powers. These spectra could be acquired in a typical time of two hours.
The resolution of the spectrometer is not high enough to give a more detailed analysis but it can show the variation of the spectra as a function of the injected power and identify the Ar lines.

At 400 W, the structure labeled Ar^{13+} is the most prominent of the highly-charged ion lines, and would certainly be a good candidate for a first attempt of high-resolution x-ray spectroscopy. The relativistic M1 line in He-like argon would be the ideal candidate for high-precision, high-resolution spectroscopy, but it is probably too weak at this stage to be observed. It should be noted that the spectrometer used in the experiment shown on Fig 8 observed the plasma through a ~500 µm diameter pinhole, as it required an entrance slit, and also a reduction of rate. A double-flat crystal instrument [17], although very inefficient, would make use of the full polarization electrode aperture, which represents a 570 fold increased intensity. Figure 8 shows the operation principle of the double crystal instrument under development in our group.

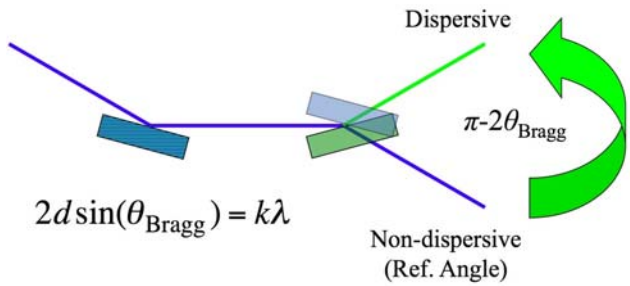

Figure 8: Operation principle of a double crystal instrument. The first crystal (left) acts like a monochromator, and by measuring the angle difference between the two positions of the second crystal the wavelength of the chosen transition can be absolutely determined.

With this instrument x-ray wavelength can be absolutely measured by angle difference measurement. The new double crystal spectrometer dedicated to x-ray measurements at ECR ion sources has the ability to rotate the whole optical table supporting the rotational stages of both crystals inside the vacuum chamber. With this the first crystal can be aligned to accept the x rays at the right Bragg angle for the line under investigation. With absolute wavelengths measurements of the lines from HCI with great accuracy these lines can serve as new x-ray standards with their very narrow features in high precision x-ray spectroscopy.

SUMMARY

We have shown our first results with the new electrostatic ion beam trap (EIBT) installed at the beam line of the SIMPA ion source. With this device we have proven trapping of highly charged ions up to O^{5+}, Ar^{13+}, Kr^{21+} and Xe^{20+}. We have also made progress with computer simulations explaining oscillations on the millisecond scale on the trapping signal.
From x-ray spectroscopic studies we have defined an average electron temperature based on the bremsstrahlung radiation that is in good agreement with other measurements at other ECRIS laboratories.

We also have reported on the progress of our double crystal spectrometer project that will provide new x-ray standards through high precision absolute wavelength measurements using highly charged ions in an ECRIS.

ACKNOWLEDGMENTS

This work has been supported by a grant from "Agence Nationale pour la Rechcherche (ANR)" number ANR-06-BLAN-0233. The Authors would like to acknowledge the assistance and encouragement from colleagues and the special work of the technical staff.

REFERENCES

[1] Zajfman D, Heber O, Vejby-Christensen L, Ben-Itzhak I, Rappaport M, Fishman R, and Dahan M 1997 Phys. Rev. A **55** R1577

[2] Dahan M, Fishman R, Heber O, Rappaport M, Altshtein N, van der Zande W J and Zajfman D, 1998 Rev. Sci. Instrum. **69** 76

[3] Wester R, Bhushan K G, Altstein N, Zajfman D, Heber O, and Rappaport M L 1999 J. Chem. Phys. **110** 11 830

[4] Knoll L, Bhushan K G, Altstein N, Zajfman D, Heber O, and Rappaport M L 1999 Phys. Rev. A **60** 1710

[5] Strasser D, Bhushan K G, Pedersen H B, Wester R, Heber O, Lafosse A, Rappaport M L, Altstein N, and Zajfman D 2000 Phys. Rev. A **61** 060705

[6] Pedersen H B, Strasser D, Heber O, Rappaport M L, and Zajfman D 2002 Phys. Rev. A **65** 042704

[7] C.Barué, M. Lamoureux, P. Briand, et al., J. Appl. Phys. **76**, 2662 (1994).

[8] R. D. Deslattes (1967) Rev. Sci. Instrum. **38** pp. 616-620

[9] C. D. Cohen, Nucl. Instrum. Meth. A **267**, 492 (1988)

[10] J J. Hubbell, S.M. Seltzer, Tech. Rep. NISTIR 5632, National Institute of Standards and Technology (1995), http://physics.nist.gov/PhysRefData/XrayMassCoef/cover.html

[11] G. Douysset, H. Khodja, A. Girard, J.P. Briand, Phys. Rev. E **61**(3), 3015 (2000)

[12] S. Biri, L. Simons, D. Hitz, Rev. Sci. Instrum. **71**, 1116 (2000)

[13] D.F. Anagnostopoulos, S. Biri, D. Gotta, A. Gruber, P. Indelicato, B. Leoni, H. Fuhrmann, L.M. Simons, L. Stin- gelin, A. Wasser et al., Nuc. Instrum. Methods A **545**, 217 (2005)

[14] D.F. Anagnostopoulos, S. Biri, V. Boisbourdain, M. Demeter, G. Borchert, J. Egger, H. Fuhrmann, D. Gotta, A. Gruber, M. Hennebach et al., Nucl. Instrum. Methods B **205**(1-4), 9 (2003)

[15] M. Trassinelli, S. Boucard, D.S. Covita, D. Gotta, A. Hirtl, P. Indelicato, O.L. Bigot, J.M.F.d. San- tos, L.M. Simons, L. Stingelin et al., Journal of Physics: Conference Series **58**, 129 (2007) http://stacks.iop.org/1742-6596/58/129

[16] P. Indelicato, S. Boucard, D.S. Covita, D. Gotta, A. Gruber, A. Hirtl, H. Fuhrmann, E.O.L. Bigot, S. Schlesser, J.M.F.d. Santos et al., Nucl. Instrum. Meth. A **580**, 8 (2007)

[17] J. W. M. DuMond, A. Hoyt, Phys. Rev. **36** p.1702 (1930)